SUBMITTED TO ApJ
Preprint typeset using LaTeX style emulateapj

# THE LUMINOSITY DEPENDENCE OF UV ABSORPTION IN AGN

ARI LAOR
Technion, Physics Dept., Haifa 32000, Israel.
laor@physics.technion.ac.il
W. N. BRANDT
The Pennsylvania State University, Dept. of Astronomy & Astrophysics, 525 Davey Lab,
University Park, PA 16802. niel@astro.psu.edu

Revised version, submitted for publication in ApJ on January 1st, 2002.

## ABSTRACT

We describe the results of a survey of the UV absorption properties of the Boroson & Green sample of AGN, which extends from the Seyfert ($M_V \simeq -21$) to the luminous quasar ($M_V \simeq -27$) level. The survey is based mostly on *HST* archival data available for $\gtrsim 1/2$ of the 87 sample objects. Our main result is that soft X-ray weak quasars (SXWQs, 10 AGN with $\alpha_{ox} \leq -2$) show the strongest UV absorption at a given luminosity, and their maximum outflow velocity, $v_{\rm max}$, is strongly correlated with $M_V$ ($r_S = -0.95$). This suggests that $v_{\rm max}$ is largely set by the luminosity, as expected for radiation-pressure driven outflows. Luminous SXWQs have preferentially low [O III] luminosity, which suggests they are physically distinct from unabsorbed AGN, while non-SXWQs with UV absorption are consistent with being drawn from the unabsorbed AGN population. We also find an indication that $v_{\rm max}/v_{\rm BLR}$ increases with $L/L_{\rm Edd}$, as expected for radiation-pressure driven outflows. This relation and the $v_{\rm max}$ vs. $M_V$ relation may indicate that the radiation-pressure force multiplier increases with luminosity, and that the wind launching radius in non-SXWQs is $\sim 10$ times larger than in SXWQs.

*Subject headings:* galaxies: active–quasars: absorption lines–X-rays: galaxies

## 1. INTRODUCTION

Fast outflows are common in AGN. The outflow properties are very different in high and low-luminosity AGN. Whereas luminous high-$z$ quasars display outflows reaching a few $10^4$ km s$^{-1}$ in $\sim 10\%$ of the objects, Seyfert galaxies display typical outflow velocities up to only $\sim 10^3$ km s$^{-1}$, but in $\sim 50\%$ of the objects. *Why are the outflow properties so different at low and high-luminosity? How do the outflow properties vary with luminosity? Are AGN with outflows normal AGN seen at a preferred angle, or are they physically distinct objects? How is the UV absorption related to X-ray absorption?* The answers bear important clues to the origin and acceleration mechanism of AGN outflows.

The largest and most systematic study of broad absorption line quasars (BALQs) was carried out by Weymann et al. (1991), using ground-based spectroscopy of $z > 1.5$ quasars. More recent well-defined samples of BALQs are emerging from other large ground-based surveys (Becker et al. 2000; Menou et al. 2001; Hall et al. 2001). However, these comprehensive studies are limited to luminous quasars. Studies of absorption in low-luminosity AGN are best done in low-$z$ objects and thus require *HST* (see Crenshaw et al. 1999 for the most comprehensive study). There are many detailed studies of various objects ranging in luminosity from Seyferts to quasars, but these are focused on understanding the absorber properties of each object and do not provide a clear comprehensive picture.

In this study we make a first step toward a uniform and systematic survey of the UV absorption properties of AGN from the Seyfert to the luminous quasar level. We primarily use archival *HST* observations of the Boroson & Green (1992; hereafter BG92) sample, which includes the 87 $z < 0.5$ Palomar-Green (PG, Schmidt & Green 1983) AGN, and extends from Seyferts at $M_V \simeq -21$ to luminous quasars at $M_V \simeq -27$. The high-quality optical data set available from BG92 allows us to explore relations between quasar absorption and emission properties known as "eigenvector 1" (EV1; BG92; Boroson 2002),[1] which are also strongly correlated with X-ray and UV emission properties (e.g., Laor et al. 1997, hereafter L97; Brandt & Boller 1999; Wills et al. 1999; Laor 2000). These correlations are particularly interesting since they may be driven by fundamental parameters, specifically the black hole mass and the accretion rate.

The UV absorption properties of some AGN from the BG92 sample have been studied by various authors (see the references in Appendix A and in Brandt, Laor, & Wills 2000; hereafter BLW, §§5, 6), and a complete census of the C IV absorption equivalent width, EW(C IV), of all BG92 AGN with sufficient quality UV spectra is provided by BLW. This study also provides a complete systematic census of the effective optical-to-X-ray spectral slope, $\alpha_{ox}$, based on *ROSAT* data.[2] The $\alpha_{ox}$ was used by BLW to define a complete sample of Soft X-ray Weak quasars (SXWQs), which includes all 10 AGN from BG92 with $\alpha_{ox} \leq -2$. The $\alpha_{ox} \leq -2$ cutoff is based on the distribution of $\alpha_{ox}$ in the BG92 sample, which suggests an apparently distinct group of SXWQs (see BLW). Since $\langle\alpha_{ox}\rangle \simeq -1.48$ in non-SXWQs (Laor et al. 1997, and §3.2 here), the 2 keV luminosity of SXWQs is suppressed by a factor of $\geq 25$ on average, compared to non-SXWQs with the same optical luminosity. BLW discovered a very strong relation between $\alpha_{ox}$ and EW(C IV), which suggests that soft X-ray weakness is due to absorption,

[1]EV1 is defined in BG92, and represents a set of correlated optical emission properties, including in particular the strength of the [O III] and Fe II emission, and the H$\beta$ line width.

[2]Note that more recent *HST* and *ASCA* observations of some of the objects indicate that in a few cases $\alpha_{ox}$ may vary significantly (e.g., Gallagher et al. 2001).

as was directly confirmed for some objects by hard X-ray spectroscopy (e.g., Gallagher et al. 1999, 2001; Green et al. 2001).

The EW(C IV) of the 10 SXWQs covers a wide range (1 – 100 Å), and although nearly all BALQs are SXWQs (e.g., Kopko, Turnshek, & Espey 1994; Green et al. 1995; Green & Mathur 1996), the converse is not true as only some of these SXWQs can be defined as BALQs (see below). *What determines if a SXWQ is a BALQ?* The purpose of this paper is to answer this question, together with some of the questions posed in the opening paragraph. The paper is organized as follows. In §2 we briefly describe the method of analysis, and in §3 we provide the absorption statistics and discuss their dependence on $M_{[\rm O\ III]}$, $M_V$, radio-loudness, emission-line strengths, and fundamental parameters. Some further open questions are discussed in §4, and the main conclusions are summarized in §5. Appenix A provides notes on individual objects, supplementing the notes in BLW, and Appendix B lists the 28 objects without intrinsic UV absorption.

## 2. METHOD

We retrieved all public Faint Object Spectrograph and High Resolution Spectrograph spectra of the BG92 AGN available in the *HST* archives, and supplemented these with the four *IUE* spectra of SXWQs presented by BLW. UV coverage of C IV and/or Ly$\alpha$+N V was obtained for 56 objects which extend from $M_V = -21.44$ to $M_V = -27.26$. Of these, 42 have *HST* coverage of both C IV and Ly$\alpha$+N V, and six have only C IV coverage. Five objects have no C IV coverage, and Ly$\alpha$+N V was used instead. In three additional objects (SXWQs) both C IV and Ly$\alpha$+N V were obtained from *IUE*.

The wavelength scale of each spectrum has been calibrated using low-ionization Galactic absorption lines (O I, C II, Si II, Al II) which are detectable in most spectra (e.g., Savage et al. 2000). We measure the intrinsic UV absorption using the C IV line since it is generally a strong absorption line, because it is relatively simple to define the emission shape in its vicinity (unlike N V), and because it is much less likely than Ly$\alpha$ to be affected by intervening systems. The absorption is parametrized here using three numbers, the absorption rest-frame equivalent width, EW(C IV), the maximum velocity of absorption, $v_{\rm max}$ (expected to be physically related to luminosity, see §3.4), and the velocity of maximum absorption, $v_{\tau,{\rm max}}$ (much less sensitive to continuum placement than $v_{\rm max}$). In some objects the C IV absorption appears only marginally significant. To verify its existence we required that the second C IV doublet component be present (if the absorption is narrow enough), and that there is a feature at the same velocity in either N V or Ly$\alpha$. In three of the five objects where C IV is not available, absorption is detected in Ly$\alpha$ and the values for Ly$\alpha$ are reported here. For the sake of brevity we use the term "C IV absorption" throughout the paper, but we use a special symbol to denote the three Ly$\alpha$ objects in the figures.

Absorption was searched for from 0 km s$^{-1}$ to 30,000 km s$^{-1}$ in blueshift with respect to the systemic redshift determined from [O III] $\lambda$5007 (provided by T. A. Boroson 2001, private communication). At velocities higher than 30,000 km s$^{-1}$ the C IV absorption may be confused with Si IV absorption, and for the sake of simplicity we avoid this velocity range. The systemic redshifts are not heliocentric, but the resulting error is smaller than the typical spectral sampling element size of $\sim 50-100$ km s$^{-1}$. The mean heliocentric velocity of the low-ionization Galactic absorption lines, used here to calibrate the wavelength scale of the *HST* spectra, is also typically well below 100 km s$^{-1}$ (e.g., Savage et al. 2000), and thus we expect our *HST* velocity calibration to be accurate to a level of $\sim$ 100 km s$^{-1}$, or better (excluding the four objects were no Galactic absorption was identified, as noted in Table 1).

The absorption EW is measured by making a linear interpolation (in log $f_\lambda$ vs. log $\lambda$) for the unabsorbed flux between the two closest continuum points judged to be unabsorbed. There is no accurate way to estimate the EW uncertainty, as it is most likely dominated by systematic errors in the continuum placement. As a rough guide we estimate the associated error is typically $\sim 10-20$%, and generally not below $\sim 0.1$ Å. Very shallow (depth$<$ 10%) and broad (width$>$ a few thousand km s$^{-1}$) absorption troughs would remain undetected in our sample.

## 3. RESULTS & DISCUSSION

### 3.1. *Absorption Frequency*

Absorption is detected in 28 of the 56 BG92 sample objects, and their EW(C IV), $v_{\rm max}$, and $v_{\tau,{\rm max}}$ values are listed in Table 1. In 21 objects the parameters are based on *HST* C IV profiles, in three on *HST* Ly$\alpha$ profiles, and in four on *IUE* C IV profiles (all SXWQs from BLW). In two of these last four the absorption is only marginally significant (PG 1011–040 and PG 2214+139, see Appendix A), and we use a special symbol to denote them in the figures. Table 1 also lists the redshift, the 3000 Å to 2 keV spectral slope, $\alpha_{ox}$, taken from BLW, $M_V$ and EW([O III]) from BG92, and the continuum luminosity at 3000 Å, based on the continuum fluxes from Neugebauer et al. (1987). A note to the table provides the Balnicity Index (BI), as defined by Weymann et al. (1991), for the five objects where BI$>$ 0.

Strong absorption, defined here as EW(C IV)$>$10 Å, is detected in 6/56 of the sample objects, of which five have BI$>$ 0, i.e. a frequency of $\sim$ 10% for BALQs/strong absorption AGN. Intermediate-strength absorption, 1 Å$<$EW(C IV)$<$10 Å, is detected in 11/56, $\sim$ 20%, and weak absorption, 0.1 Å$<$EW(C IV)$<$1 Å, in 11/56, $\sim$ 20%. The remaining 50% have no detectable absorption, i.e. EW(C IV) $\lesssim$ 0.1 Å, and they are listed in Appendix B. However, these frequencies may be subject to significant systematic errors since the available subsample of 56 BG92 AGN is not complete or well-defined in any way, and some of the objects in it were observed because of their absorption properties.

Figure 1 shows the absorption profiles for the 10 SXWQs. Figure 2 shows the absorption profiles for the 11 non-SXWQs with intermediate UV absorption, and Figure 3 shows the 11 objects with weak absorption.

### 3.2. *EW(C IV) vs.* $\alpha_{ox}$

Figure 4 presents a revised version of Fig. 4 from BLW, as some of the EW(C IV) values found here are somewhat different from those listed in BLW (see Appendix A). As discussed in BLW, all the SXWQs have intermediate-to-strong UV absorption (with possible exceptions for PG 1011–040 and PG 2214+139), and all the objects with strong UV absorption are SXW, consistent with the earlier result that practically all BALQs are SXW.

The second notable group is the non-SXWQs with intermediate UV absorption (marked by stars in Fig. 4). The seven objects in this group are also intermediate in their $\alpha_{ox}$, having $\langle\alpha_{ox}\rangle = -1.68 \pm 0.11$. They have almost no overlap with the $\alpha_{ox}$ of the 11 objects with weak UV absorption, which have $\langle\alpha_{ox}\rangle = -1.49 \pm 0.08$. As noted in BLW, X-ray spectra available for some of these intermediate objects suggest intrinsic X-ray absorption features as well, but the S/N is generally too low to identify the features (excluding PG 1114+445 which shows what appears to be a warm absorber edge, George et al. 1997). These intermediate objects are relatively X-ray bright and would be interesting to explore with higher resolution X-ray spectroscopy.

Nearly all objects with no UV absorption have a "normal" $\alpha_{ox} \sim -1.5$. The two significant exceptions are PG 1259+593 and PG 1543+489, which have significantly steeper $\alpha_{ox}$. Interestingly, these two objects also have very unusual UV line profiles (very broad, highly blueshifted, and very asymmetric), which may be related to their unusual $\alpha_{ox}$.

### 3.3. *The $M_{[\mathrm{O\ III}]}$ distribution*

As pointed out by BLW (see Fig. 3 there), SXWQs tend to lie toward the weak-[O III] end of the BG92 EV1 (see §1). This result is consistent with the findings of Boroson & Meyers (1992) that low-ionization BALQs are much more common in low-EW([O III]) AGN, and the similar finding of Turnshek et al. (1997) for normal BALQs, as both of these types of BALQs are generally SXW. BLW further showed that the difference in the [O III] luminosities of SXW AGN vs. non-SXW AGN is more significant than the difference in their EW([O III]). Are non-SXW AGN with UV absorption also more common at low [O III] luminosities? We first take a closer look at the [O III] luminosities of SXWQs and then address this question (the difference in EW([O III]) is discussed in §3.5).

Figure 5 shows the positions of the 56 AGN studied here in the $M_{[\mathrm{O\ III}]}$ vs. $M_V$ plane, where $M_{[\mathrm{O\ III}]} \equiv M_V - 2.5\log$ EW([O III]) (defined in BG92) is used here as a measure of the [O III] luminosity. Radio-loud and radio-quiet AGN are shown separately in Fig. 5 since their $M_{[\mathrm{O\ III}]}$ and $M_V$ distributions are significantly different (see Table 5 in BG92). All 9 radio-quiet SXWQs lie at $M_{[\mathrm{O\ III}]} > -27$, where they form $\sim 35\%$ (9/26) of the population. The Poisson probability that the true fraction of SXWQs at $M_{[\mathrm{O\ III}]} < -27$ is also $\sim 35\%$ is $7.8 \times 10^{-3}$. PG 1004+130 is the only SXWQ of the 14 radio-loud AGN in our sample, and it also lies at the bottom of the radio-loud $M_{[\mathrm{O\ III}]}$ distribution. A KS test for the combined sample of SXWQs gives a probability of 1.5% that the 10 SXWQs and the 28 AGN with no UV absorption are drawn from the same $M_{[\mathrm{O\ III}]}$ distribution. In this combined sample the fraction of SXWQs at $M_{[\mathrm{O\ III}]} < -27$ is $\sim 3\%$ (1/30) (the single object is PG 1004+130), and the Poisson probability that the true fraction is $\sim 35\%$, as found for $M_{[\mathrm{O\ III}]} > -27$, is $3.2 \times 10^{-4}$.

Inspection of Fig. 5 suggests that the difference in the $M_{[\mathrm{O\ III}]}$ distributions of SXWQs and non-SXWQs is mostly driven by the more luminous AGN. Indeed, a KS test for the complete BG92 sample of 87 AGN gives a probability of 1.2% that the 4 SXWQs and 20 non-SXWQs more luminous than $M_V = -25$ are drawn from the same $M_{[\mathrm{O\ III}]}$ distribution, while for AGN less luminous than $M_V = -25$ the probability for that is 18% (6 SXWQs and 57 non-SXWQs).

In contrast to SXWQs, non-SXWQs with intermediate and weak UV absorption are not significantly different in their $M_{[\mathrm{O\ III}]}$ distribution from unabsorbed AGN (see Fig. 5). The KS test gives a probability of 39% that intermediately-absorbed and unabsorbed AGN are drawn from the same distribution, and a corresponding probability of 97% for the weakly absorbed AGN. *What do these $M_{[\mathrm{O\ III}]}$ distributions imply?*

The [O III] emission is most likely isotropic (e.g., Kuraszkiewicz et al. 2000 and references therein). Thus, as BLW pointed out (§8 there), the weakness of [O III] in SXWQs strongly suggests they are physically distinct from normal $\alpha_{ox}$ quasars, as suggested by Boroson & Meyers (1992) and Turnshek et al. (1997) for low-ionization and normal BALQs. The distributions in Fig. 5 suggest then that SXWQs, in particular the luminous ones, are physically distinct from AGN with no UV absorption, but that AGN with intermediate to weak UV absorption are consistent with being drawn from the unabsorbed AGN population.

The low [O III] luminosities of luminous SXWQs argue then against the common interpretation in which BALQs are normal quasars seen edge on (e.g., Weymann et al. 1991). An alternative interpretation is that there is a range of covering factors of the obscuring material in AGN, and this covering factor strongly influences $M_{[\mathrm{O\ III}]}$. For example, the numbers found in our incomplete (and possibly biased) study would suggest that in AGN with $M_{[\mathrm{O\ III}]} < -27$ $\sim 57\%$ of the "sky" is clear, $\sim 20\%$ is covered by low-column density clouds, $\sim 20\%$ by intermediate-column density clouds, and only $\sim 3\%$ by high-column density clouds producing strong UV and X-ray absorption, while in $M_{[\mathrm{O\ III}]} > -27$ AGN $\sim 40\%$ of the "sky" is clear, $\sim 25\%$ is covered by low-to-intermediate column density clouds, and $\sim 35\%$ is covered by high-column density clouds (see Table 2). Note that the clouds' covering factors may be underestimated if the optical continuum emission of UV absorbed quasars is suppressed (Goodrich 1997; Krolik & Voit 1998), as suggested by the recent composite spectra presented by Brotherton et al. (2001).

### 3.4. *The Luminosity Dependence*

What determines if a SXWQ is a BALQ? The answer appears to be remarkably simple. Figure 6 shows the distribution of EW(C IV) and of $v_{\max}$ vs. $M_V$ for all 28 absorbed AGN. SXWQs have a higher EW(C IV) and a higher $v_{\max}$, at any given luminosity, than intermediate and weak UV absorption AGN. In addition, both EW(C IV) and $v_{\max}$ of the SXWQs are strongly correlated with $M_V$. The Spearman rank order correlation coefficient, $r_S$, and its significance level, Pr, for the EW(C IV) vs. $M_V$ correlation are $-0.93$ and $1.1 \times 10^{-4}$, and for the $v_{\max}$ vs. $M_V$ correlation they are $-0.95$ and $2.3 \times 10^{-5}$. A least-squares fit to the SXWQs gives EW(C IV)$\propto L^{0.68\pm0.18}$, and $v_{\max} \propto L^{0.62\pm0.08}$. Only five objects in our sample are "true" BALQs, using the Weymann et al. (1991) definition of BI$> 0$ (see the note to Table 1), and these are also the five most luminous SXWQs. Thus, BALQs are simply luminous SXWQs.

On the other hand, for non-SXWQs there is no significant luminosity dependence of either EW(C IV) or $v_{\max}$ (there may be a negative trend of EW(C IV) with $M_V$ for the low-EW(C IV) AGN, but the significance is $< 2\sigma$). The differences in the $M_V$ dependence for SXWQs and non-SXWQs suggests that the UV absorption in these two populations occurs in physically different classes of absorbers.

The strong luminosity dependence of $v_{\max}$ is consistent with some radiation-pressure acceleration scenarios. For example, if the BAL outflow is launched by radiation-pressure acceleration on optically thin clouds moving at some Keplerian velocity $v_{\rm Kep}$, at some radius $R$, then the terminal outflow velocity is

$$v_{\rm ter} \simeq v_{\rm Kep} \times \sqrt{\Gamma L/L_{\rm Edd}},$$

where $\Gamma$ is the force multiplier, which depends on the opacity sources in the gas (dust, lines, or bound-free absorption), and is assumed to remain constant throughout the flow. Since

$$v_{\rm Kep} \propto \sqrt{M_{\rm BH}/R} \quad \text{and} \quad L_{\rm Edd} \propto M_{\rm BH}$$

we get that

$$v_{\rm ter} \propto \sqrt{\Gamma L/R}.$$

Thus, in an object with a given $L$, the maximum terminal outflow velocity is obtained for a flow which starts at the minimum launching radius, $v_{\rm max} = v_{\rm ter}(R_{\rm min})$. If the main opacity source is dust (Scoville & Norman 1995), then the minimum radius where grains survive is

$$R_{\rm min} \propto L^{1/2},$$

which is just outside the radius of the Broad Line Region (BLR, Laor & Draine 1993). Alternatively, the outflow may be driven by line opacity and be launched from $R_{\rm min} = R_{\rm BLR}$. However, since $R_{\rm BLR} \propto L^{\sim 1/2}$, as both observations (Kaspi et al. 2000), and theoretical arguments (Netzer & Laor 1993) indicate, then qualitatively similar outflows could be obtained for dust and line driving. If, in addition, $\Gamma$ is independent of $L$ (e.g., if the grain size distribution, composition, and dust/gas ratio, or the gas ionization level, are the same in all objects) we obtain that

$$v_{\rm max} \propto L^{1/4},$$

i.e. a pure luminosity dependence (e.g., Arav, Li, & Begelman 1994, eq. 3.3; Scoville & Norman 1995, eq. 6). The observed slope $0.62 \pm 0.08$ is significantly steeper than this simplified model prediction of 0.25. The difference may not be significant if the small slope uncertainty is just a coincidence due to the small sample size. However, it could also be due to a failure of one or more of the above assumptions. For example, if $R_{\rm min}$ is independent of $L$ then $v_{\rm max} \propto L^{1/2}$ (e.g., Weymann, Turnshek, & Christiansen 1985). If the flow is launched at $R_{\rm min} \propto L^{1/2}$, then the observed slope implies empirically that $\Gamma$ is not independent of $L$, but rather $\Gamma \propto L^{0.74}$.

A correlation analysis using $v_{\tau,\rm max}$ instead of $v_{\rm max}$ yields very similar or slightly stronger correlations, both here and in the following sections, and for the sake of brevity we do not report these results. Exclusion of the two lower quality *IUE*-based data points of PG 1011−040 and PG 2214+139, also generally yields similar or somewhat stronger correlations, and are also not reported here and below.

### 3.5. *Dependence on other Emission Properties*

BG92 have shown significant correlations among optical emission-line parameters, in particular among the H$\beta$ width and asymmetry, $M_{\rm [O\ III]}$, [O III] to H$\beta$ peak flux ratio, and Fe II/H$\beta$ flux ratio (some of the dominant components of EV1 in BG92). These correlations extend to the X-ray (e.g., L97) and to the UV (e.g., Wills et al. 1999), and may be due to systematic changes in the BLR and NLR properties with increasing $L/L_{\rm Edd}$. *Are the UV absorption properties of SXWQs related to any of the BG92 optical emission-line properties?*

Figure 7 shows that EW(C IV) and $v_{\rm max}$ are significantly correlated with EW([O III]) for the SXWQs (in addition to the low [O III] luminosities of SXWQs, §3.3), and there appears to exist an overall upper "envelope" of decreasing EW(C IV) and $v_{\rm max}$ with increasing EW([O III]), although there is no significant correlation for the intermediate and weak absorption AGN. A somewhat weaker correlation (Pr=$5 \times 10^{-3}$) of EW(C IV) and $v_{\rm max}$ was found with EW(He II 4686), and none of the other emission-line parameters tabulated by BG92 shows any significant correlation with either EW(C IV) or $v_{\rm max}$.

The rather strong correlation between EW([O III]) and $v_{\rm max}$, together with the lack of correlation with other EV1 emission-line parameters is intriguing. *Is there a direct physical link between $v_{\rm max}$ and* EW([O III])? Possible direct links could be a greater destruction of NLR clouds by higher velocity outflows, or an increasing obscuration of the NLR due to interactions of a faster outflow with nearby dense clouds which increases the scale height of the obscuring gas. However, there is an indication that the relation between EW([O III]) and $v_{\rm max}$ may be indirect. There is a very strong correlation of EW([O III]) with $M_V$ for the SXWQs ($r_S = 0.91$, Fig. 5), and there is also a very strong correlation of $v_{\rm max}$ with $M_V$ ($r_S = -0.95$, Fig. 6). Thus, the somewhat weaker correlation of EW([O III]) with $v_{\rm max}$ ($r_S = -0.90$) may be a secondary effect, as partial correlation analysis indicates (using eq. 27 in Kendall & Stuart 1977), and it does not necessarily imply a direct physical link. However, the origin of the highly significant EW([O III]) vs. $M_V$ correlation in SXWQs (Pr=$2.8 \times 10^{-4}$) remains to be understood. AGN in general show a trend of decreasing EW([O III]) with increasing luminosity (see Fig. 3 in BLW), but with a very broad scatter. SXWQs populate the lower boundary of the EW([O III]) vs. $M_V$ distribution of AGN, and for some unknown reason this lower boundary decreases with increasing luminosity, creating the observed correlation.

Earlier studies suggested that BALQs are restricted to the radio-quiet quasar population, but recent deep radio surveys are finding that BALQs occur with about equal frequency in radio-loud and radio-quiet quasars (Becker et al. 2000; Menou et al. 2001). However, the UV absorption strength and velocity extent may still be larger in radio-quiet quasars, in particular when compared to the most radio-loud quasars ($R > 100$, Becker et al. 2001). Figure 8 shows the dependence of EW(C IV) and $v_{\rm max}$ on the radio/optical flux ratio in our sample. KS tests indicate that the eight radio-loud and 20 radio-quiet AGN in our sample are consistent with being drawn from the same distributions of EW(C IV) and $v_{\rm max}$ (Pr=0.49 for both). The trend noted in earlier studies may become statistically significant if a larger sample is studied.

### 3.6. *Dependence on Fundamental Parameters*

The black hole mass ($M_{\rm BH}$) in AGN can be estimated using the H$\beta$ FWHM ($v_{\rm BLR}$) and the size of the H$\beta$ emitting region ($R_{\rm BLR}$) obtained from reverberation mapping, or from the BLR size-luminosity relation (e.g., Kaspi et al. 2000), with the assumption of virialized motion in the BLR (e.g. Peterson, & Wandel 2000), giving $M_{\rm BH}({\rm H}\beta) = v_{\rm BLR}^2 \times R_{\rm BLR}/G$, or

$$m_9 = 0.18 v_{3000}^2 L_{46}^{1/2},$$

where $m_9 \equiv M_{\rm BH}({\rm H}\beta)/10^9 M_\odot$, $v_{3000} \equiv v_{\rm BLR}/3000$ km $^{-1}$, and $L_{46}$ is the bolometric luminosity in units of $10^{46}$ erg s$^{-1}$ (e.g. Laor 1998). Since the Eddington luminosity in units of $10^{46}$ erg s$^{-1}$ is $L_{\rm Edd} = 12.5 m_9$, the above relation implies

$$L/L_{\rm Edd} = 0.44 v_{3000}^{-2} L_{46}^{1/2}.$$

Such estimates are potentially significantly uncertain (e.g., Krolik 2001); however, recent studies have shown that the H$\beta$-based black hole mass estimate in AGN is correlated with the host bulge luminosity and with the host bulge stellar velocity dispersion, as found for nearby non-active galaxies (Laor 1998; Ferrarese et al. 2001; Gebhardt et al. 2000). This indicates that $M_{\rm BH}({\rm H}\beta)$ provides a reasonably accurate estimate of the true $M_{\rm BH}$ (to within a factor of 2–3), and it opens up the possibility of looking for correlations of various observed properties with the underlying fundamental parameters, $M_{\rm BH}$ and $L/L_{\rm Edd}$.

The simplified radiation-pressure driven outflow scenario (§3.4) implies that if the outflow is launched at $R_{\rm min} \simeq R_{\rm BLR}$, then

$$v_{\rm max}/v_{\rm BLR} \simeq \sqrt{\Gamma L/L_{\rm Edd}},$$

where we assume $v_{\rm Kep} \simeq v_{\rm BLR}$. Figure 9 shows there indeed exists an apparently significant correlation between the observed $v_{\rm max}/v_{\rm BLR}$ and $L/L_{\rm Edd}$. The value of $L/L_{\rm Edd}$ for each object is obtained using the H$\beta$ FWHM from BG92, assuming $L_{46} = 8.3\nu L_\nu(3000\ \text{Å})$ (Laor 1998), where $\nu L_\nu(3000\ \text{Å})$ is listed in Table 1. The strength of the correlation for the combined sample of 24 AGN with significant outflow velocity[3] is $r_S$=0.76 (Pr=$1.9\times10^{-5}$). The other option mentioned in §3.4 that $R_{\rm min}$ is a constant (independent of $L$) would not imply the correlation seen in Fig. 9.

As argued above (§§3.3, 3.4), the UV absorbers in SXWQs and non-SXWQs are likely to be different, so we repeated the analysis for the two populations separately. A marginally significant correlation is still present for the 10 SXWQs ($r_S$ = 0.72, Pr=$1.9\times10^{-2}$), and a significant correlation is present for the 14 non-SXWQs ($r_S$=0.85, Pr=$1.6\times10^{-4}$). The best-fit slopes for the two populations are very similar; for SXWQs, $v_{\rm max}/v_{\rm BLR} \propto (L/L_{\rm Edd})^{0.91\pm0.24}$; and for non-SXWQs, $v_{\rm max}/v_{\rm BLR} \propto (L/L_{\rm Edd})^{0.83\pm0.16}$. Under the simplified outflow scenario described above these slopes imply that $\Gamma$ must increase with $L/L_{\rm Edd}$. Specifically, the above relations imply $\Gamma \propto (L/L_{\rm Edd})^{0.82}$ for SXWQs, and $\Gamma \propto (L/L_{\rm Edd})^{0.66}$ for non-SXWQs. This luminosity dependence of $\Gamma$ is comparable to $\Gamma \propto (L/L_{\rm Edd})^{0.68}$ suggested by the $v_{\rm max}$ vs. luminosity relation (§3.4), which is independent of the observed values of $v_{\rm BLR}$.

The non-SXWQs in Fig. 9 fall on average a factor of $\sim 3$ below the SXWQs. A possible interpretation is that the UV absorbing outflows in non-SXWQs are launched at $\sim 10$ times larger distance than in SXWQs. At this larger distance $v_{\rm Kep}$, and thus the resulting $v_{\rm max}$ (see §3.4), are a factor of $\sim 3$ smaller, at a given $L/L_{\rm Edd}$. A possible alternative explanation is that the launching radius is the same in all objects, but in non-SXWQs the outflows become fully ionized before reaching $v_{\rm max}$ due to their higher X-ray flux. This alternative cannot be ruled out, but we note that intermediate $\alpha_{ox}$ AGN do not have intermediate $v_{\rm max}$, as one may expect given their apparently intermediate strength ionizing radiation, but rather the same $v_{\rm max}$ as of normal $\alpha_{ox}$ AGN of the same $M_V$ (Fig. 6). This alternative can be directly tested by looking for higher ionization lines (e.g. O VI, Ne VIII) which should display a higher $v_{\rm max}$.

Since $\Gamma \simeq (v_{\rm max}/v_{\rm BLR})^2/(L/L_{\rm Edd})$ (§3.4), then Fig. 9 together with our assumed outflow mechanism suggest that $\Gamma \sim 50-100$ in SXWQs with $L \sim L_{\rm Edd}$. Optically thin outflows with $N_{\rm H} \leq 10^{21}$ cm$^{-2}$ driven by dust or resonance-line opacity can reach $\Gamma \sim 1000$ (e.g., Arav et al. 1994; Scoville & Norman 1995), but such outflows are too thin to produce the observed X-ray absorption if their metal abundance is solar. An optically thick absorber which absorbs all incident continuum photons can reach at most $\Gamma \leq 1.5\times10^{24}/N_{\rm H}$, and thus a flow with $\Gamma \gtrsim 50$ would imply $N_{\rm H} \lesssim 10^{22}$ cm$^{-2}$, which is optically thin above 1.5 keV (i.e. cannot make an AGN SXW). Our estimates of $\Gamma$ can probably be off by an order of magnitude, but if SXWQs with UV outflows having $\Gamma \gtrsim 50$ do exist then the large column density X-ray absorber of SXWQs should not be part of this outflow, but rather should form a "heavy" non-outflowing "filter" for the the UV absorbing outflow. However, if the X-ray absorber is found to have the same dynamics of the UV outflow, then the X-ray absorber must be very "light", implying a metallicity well above solar (i.e., having little H and He which constitute most of the mass, but do not contribute much to the X-ray opacity).

The $v_{\rm max}/v_{\rm BLR}$ vs. $L/L_{\rm Edd}$ relation is subject to one major caveat. The two quantities are not determined independently, but rather both depend on $v_{\rm BLR}$. Is the observed relation physically meaningful, or is it just a secondary effect due to the strong correlation of $v_{\rm max}$ with $L$ coupled with the inclusion of $v_{\rm BLR}$ in both the $x$ and $y$ coordinate parameters? There is no conclusive answer to this question. However, there is an indirect indication that the $v_{\rm max}/v_{\rm BLR}$ vs. $L/L_{\rm Edd}$ relation is real. This is provided by the lower panel of Fig. 9 which shows the relation of $v_{\rm max}/v_{\rm BLR}$ vs. $M_{\rm BH}$. The correlation of $v_{\rm max}/v_{\rm BLR}$ with $M_{\rm BH}$ is much weaker, although the secondary effect mentioned above should affect this correlation just as well. We carried out additional tests replacing $v_{\rm BLR}$ with an unrelated optical emission-line parameter from BG92 (e.g., EW([O III]), $R$, $z$), which served as a mock "$v_{\rm BLR}$", and tested the strength of the new mock $v_{\rm max}$/"$v_{\rm BLR}$" with the new mock $L$/"$L_{\rm Edd}$" and "$M_{\rm BH}$". The results were either a strong correlation of $v_{\rm max}$/"$v_{\rm BLR}$" with both $L$/"$L_{\rm Edd}$" and "$M_{\rm BH}$", when "$v_{\rm BLR}$" had a large range of values in the sample, or no significant correlation with both parameters, when "$v_{\rm BLR}$" had a small range. Thus, the fact that $v_{\rm max}/v_{\rm BLR}$ is significantly correlated with $L/L_{\rm Edd}$, but not with $M_{\rm BH}$, provides an indirect indication we are detecting a real physical effect. This result is also consistent with our theoretical expectation that $v_{\rm max}/v_{\rm BLR}$ and $M_{\rm BH}$ should not be directly related (the observed marginally significant correlation could be induced the correlation of $M_{\rm BH}$ and $L/L_{\rm Edd}$ which has $r_S = -0.66$ in our sample).

## 4. SOME FURTHER QUESTIONS

### 4.1. Are there AGN with strong UV absorption and no X-ray absorption?

As shown in Fig. 4, there appears to exist a well-defined upper envelope to the EW(C IV) vs. $\alpha_{ox}$ distribution, and thus it appears to be impossible to have strong UV absorption without strong X-ray absorption. This result is not trivial as one may imagine a low-column density absorber ($N_{\rm H} \sim 10^{20}$ cm$^{-2}$) which can produce very strong UV absorption (EW$\gg$ 10 Å), but essentially no X-ray continuum absorption. *Why do such absorbers not exist?* A possible answer is provided by the model of Murray et al. (1995), where a strong suppression of the ionizing continuum is essential to prevent the UV absorbing outflow from becoming fully ionized. If true, then traces of absorption by highly ionized gas (e.g., in O VI, Ne VIII) may still be detected at higher outflow velocities in intermediate $\alpha_{ox}$ AGN.

### 4.2. Are all intermediate-strength UV absorbers the same?

As described in §§3.3,3.4, the different $M_{\rm [O\ III]}$ distributions of SXWQs and non-SXWQs, in particular at $M_V < -25$, and

[3] The four objects with upper limits in Fig. 9 show no significant outflow ($v_{\rm max} \leq 100$ km s$^{-1}$) and are not included in the analysis since the absorption most likely originates in gas far from the nucleus.

their different dependence of $v_{\rm max}$ on $M_V$, suggest that the UV absorption in SXWQs and non-SXWQs arises in physically different types of absorbers. If true, then although both SXWQs and non-SXWQs can show similar intermediate-strength UV absorption, higher quality UV spectroscopy could reveal differences in the absorber physical properties (e.g., covering factors, optical depths, abundances, depletions). Such differences would provide important clues about the nature of the UV and X-ray absorbers.

### 4.3. Are the X-ray and UV absorbers the same?

The simplest interpretation of the strong link between EW(C IV) and $\alpha_{ox}$ (BLW; Fig. 4) is that the X-ray and the UV absorption arise in the same absorber. Simple estimates of the UV column densities in BALQs assuming optically thin absorption imply column densities of $N_{\rm H} \sim 10^{19} - 10^{20}$ cm$^{-2}$, which are highly discrepant with the X-ray deduced column densities of $\sim 10^{23} - 10^{24}$ cm$^{-2}$. Higher quality UV spectroscopy established the importance of UV line saturation and partial covering (Kwan 1990; Korista et al. 1992; Arav 1997; Hamann 1998), and thus increased the implied UV column densities by one to possibly two orders of magnitude. However, a large discrepancy still remains in the best-studied BALQ (Arav et al. 2001 vs. Mathur et al. 2000) and in the best-studied Seyfert absorber (Kraemer et al. 2001).

The models of Murray et al. (1995) and Murray & Chiang (1995) suggest that the X-ray absorbing gas lies at the inner low-velocity part of the flow and shields the UV outflow from ionizing photons. However, if the outflow is highly clumped and is driven by radiation pressure on dust (Scoville & Norman 1995) or by other mechanisms (e.g., Begelman, de Kool & Sikora 1991), then such shielding may not be necessary. Thus, an observational determination of the relation between the UV and X-ray absorbers may allow discrimination between different acceleration models.

If the X-ray and UV absorbers are the same then, apart from a similar column density, they should also share the same kinematics. The available UV spectroscopy allows an accurate determination of the outflow kinematics but typically only weak constraints on the column density due to partial-covering and line-saturation effects, while the opposite is true for the available low-resolution X-ray spectroscopy. This problem can be alleviated, at least in part, in two ways. On the UV side, more accurate column densities can be obtained through high-quality spectroscopy of low-luminosity SXWQs, where the low outflow velocities allow one to resolve various absorption doublets, and thus better constrain the UV absorbing column density (e.g., PG 1351+64, Zheng et al. 2001). On the X-ray side, more accurate kinematic constraints can be obtained through X-ray grating spectroscopy of relatively X-ray bright SXWQs, where the outflow velocities should be fairly easy to resolve if they are similar to the observed UV velocities, even if the S/N is not very high (e.g., PG 2112+059, Gallagher et al. 2001). The intermediate X-ray and UV absorption AGN (Figs. 2, 4) could be the optimal objects for applying the absorber kinematics "identity test"; they are not as heavily absorbed in the X-rays as SXWQs are, their UV absorption is generally narrow enough to allow doublet resolution, but the outflow velocity is large enough to be resolved with X-ray grating spectroscopy. Such tests are now being done for nearby bright Seyfert galaxies with relatively weak UV and X-ray absorption (e.g., Kaspi et al. 2001), they may be possible for the intermediate objects (with a fairly large investment of time), and they may be extended to "proper" SXWQs in the future when larger collecting area X-ray telescopes become available.

### 4.4. What controls the outflowing column density?

The results presented here suggest that $v_{\rm max}$ is largely set by the luminosity, as some radiation-pressure scenarios suggest. In a source with a given $L/L_{\rm Edd}$, radiation pressure can just overcome gravity and start a radially accelerating optically thick outflow for $N_{\rm H} = 1.5 \times 10^{24} fL/L_{\rm Edd}$ cm$^{-2}$, where $f$ is the fraction of flux absorbed by the outflow from the total incident flux. For example, objects with $fL/L_{\rm Edd} \lesssim 0.01$ should not be able to drive an outflow with $N_{\rm H} > 1.5 \times 10^{22}$ cm$^{-2}$ and thus cannot produce a hard X-ray absorbing outflow ($\tau > 1$ at 2 keV). Combined X-ray and UV spectroscopy may allow us to measure the $N_{\rm H}$ of the outflow and test if it is indeed set by $fL/L_{\rm Edd}$.

### 4.5. Why are SXWQs with luminous [O III] rare?

As discussed in BLW and in §3.3, SXWQs are $\sim 10$ times more common in AGN with lower [O III] luminosity ($M_{\rm [O\ III]} > -27$) compared to AGN with luminous [O III] ($M_{\rm [O\ III]} < -27$), and the difference in $M_{\rm [O\ III]}$ distribution is most apparent for luminous AGN ($M_V < -25$). Since the measured luminosity of [O III] is most likely not inclination dependent, this implies the existence of "luminous [O III]" AGN which for some reason are only rarely SXW. Do these AGN just have a $\sim 10$ times lower covering factor of high-column density clouds ($N_{\rm H} \geq 10^{22}$ cm$^{-2}$) capable of X-ray absorption (§3.1)? Most likely not since models of the BLR indicate that $N_{\rm H} > 10^{22}$ cm$^{-2}$ clouds are required to produce the low-ionization lines (e.g., Netzer 1990), which are present at about comparable strengths in both low and high [O III] luminosity AGN. A possible alternative explanation, which also physically relates the X-ray absorption to the weakness of [O III], is that luminous [O III] AGN do not lack high-column density clouds, but rather lack high-column density clouds with a low dust/gas ratio. For some reason, some AGN may have in addition to the normal BLR gas component, another high-column density component with a low dust/gas ratio[4] covering a large solid angle (a strong wind where the dust is mostly destroyed?), through which an AGN would appear SXW, and this component may also filter much of the ionizing radiation from reaching the NLR, thus explaining why the [O III] luminosity is low. If true, then this large solid angle NLR obscuring material may also have other observational consequences, such as on the IR spectral energy distribution and on the optical polarization.

## 5. CONCLUSIONS

We describe the results of a study of the C IV absorption properties of AGN extending from the Seyfert level ($M_V \simeq -21$) to the luminous quasar level ($M_V \simeq -27$). The study is based on spectra of an incomplete subset of 56 AGN from the 87 BG92 AGN, mostly extracted from the *HST* archives. The main results are the following:

1. About 10% of the objects show strong (EW>10 Å) C IV absorption, $\sim 20\%$ show intermediate-strength (1 Å–10 Å) absorption, $\sim 20\%$ show weak (0.1 Å–1 Å) absorption, and $\sim 50\%$ show no (<0.1 Å) absorption.

[4] The composite spectrum of Brotherton et al. 2001 suggests some UV reddening in BALQs, and thus a dust column of $\sim 10^{21}$ cm$^{-2}$, which is $\sim 10^{-2} - 10^{-3}$ of the column expected based on the X-ray absorption and a normal Galactic dust/gas ratio.

2. SXWQs are $\sim 10$ times more common at $M_{[\mathrm{O\,III}]} > -27$ compared to $M_{[\mathrm{O\,III}]} < -27$, but the frequency of UV absorption in objects without strong X-ray absorption is independent of $M_{[\mathrm{O\,III}]}$. This indicates that UV absorption without strong soft X-ray absorption may be purely an inclination effect, but apparently higher column UV + soft X-ray absorption (yet without much optical extinction), as also seen in BALQs, occurs in a physical component present only in certain types of AGN.

3. SXWQs have a higher EW(C IV) and $v_{\mathrm{max}}$ at a given $M_V$ than UV-only absorbed AGN, and both parameters in SXWQs are strongly correlated with $M_V$ ($r_S = -0.93$ and $-0.95$). Thus, luminous SXWQs are BALQs, and lower luminosity SXWQs have "mini-BALs" or "associated absorbers". The observed dependence $v_{\mathrm{max}} \propto L^{0.62\pm0.08}$ is steeper than expected for constant-$\Gamma$, radiation-pressure driven outflows launched at $R \sim R_{\mathrm{BLR}}$. This may indicate that $\Gamma$ increases with luminosity.

4. There is an indication that the relative outflow velocity, $v_{\mathrm{max}}/v_{\mathrm{BLR}}$, increases with $L/L_{\mathrm{Edd}}$ for all AGN, and that the wind in non-SXWQs is launched at $\sim 10$ times the launching radius in SXWQs.

The results presented here are based on UV spectra of 56 of the BG92 AGN, a few of which have only low-quality spectra. To establish the strength and statistical significance of these results it is important to obtain high-quality UV coverage of the complete BG92 sample of 87 AGN. This survey, together with the BLW study, will establish complete UV + soft X-ray coverage of the sample. This can then be followed by detailed UV and X-ray spectroscopy of all the "interesting" AGN, which may lead to solutions of some of the above questions. In particular, the class of "intermediate" UV and X-ray absorption AGN (seven identified here, Fig. 2) may be especially suitable for studying the relation of the UV and X-ray absorbers.

This first complete UV survey of low-$z$ AGN, together with ground-based surveys of high-redshift AGN samples, will also allow one to explore if there is significant evolution in AGN absorption properties with $z$. A complete survey is a resource-intensive approach but, unlike the study of individual AGN, will allow one to draw conclusions about the general optically selected AGN population. In addition, it is important to define a significantly larger complete sample of SXWQs (e.g., Risaliti et al. 2001) to test the strength and significance of the relations described above.

We thank Todd Boroson for providing us with accurate redshifts for all objects in the BG92 sample, and Bev Wills and Sarah Gallagher for their helpful comments. We also thank the referee for a very detailed and helpful report. This research was supported by grant # 209/00-11.1 of the Israel Science Foundation to A.L. and NASA LTSA grant NAG5-8107 to W.N.B.

## APPENDIX

### A. NOTES ON INDIVIDUAL OBJECTS

Relevant notes on some of the objects appear in BLW (§§5,6). Here we provide additional notes, mostly on objects with weak C IV absorption.

0003+158– BLW note EW(C IV)=0.8 Å for this object, which refers to the $z = 0.366$ metal absorber noted by Jannuzi et al. (1998, hereafter J98). Since the associated Ly$\alpha$ line is unresolved (FWHM$<$ 250 km s$^{-1}$), the velocity shift of the system is very large ($v = -17,500$ km s$^{-1}$), and the higher order Lyman series lines indicate a (partially) optically thin absorber, this is likely to be an intervening system and we adopt here EW(C IV)=0 Å. However, we cannot rule out an intrinsic narrow high-velocity system, as suggested in some high-redshift quasars (e.g., Jannuzi et al. 1996; Hamann, Barlow, & Junkkarinen 1997; Richards et al. 1999), though the absorption in the more secure such cases is significantly broader than 250 km s$^{-1}$.

0007+106– *HST* did not observe C IV. There may be very weak N V absorption (EW$\sim$ 0.2 Å), as also suspected by Crenshaw et al. 1999 (§B1 there). The Ly$\alpha$ EW used here is likely an overestimate of the EW(C IV). No significant X-ray absorption is seen with *ROSAT* (Wang et al. 1996).

0050+124– Weak absorption in Ly$\alpha$, N V, and C IV was noted by L97 and Crenshaw et al. (1999). A closer inspection reveals also the Si IV$\lambda\lambda$1393.8,1402.8 doublet in absorption at the same velocity shift of $-1850$ km s$^{-1}$. Small excess absorption may be present in soft X-rays (Boller, Brandt & Fink 1996).

0844+349– *HST* did not observe C IV. Wang et al. (2000) noted the $v \sim 0$ km s$^{-1}$ absorption system in Ly$\alpha$. The N V absorption is weak (EW$\sim$ 0.1 Å), but both doublet components appear to be present. Wang et al. suggest in addition that the absorption at observed-frame 1260.4 Å (rest-frame $-7770$ km s$^{-1}$) is too strong and too broad to be just due to Galactic Si II$\lambda$1260.4 absorption and conclude there is intrinsic Ly$\alpha$ absorption in this feature as well. However, the Galactic C II$\lambda$1335 absorption has a very similar profile (see Fig. 3), which suggests the 1260.4 Å feature is pure Galactic absorption. There is also evidence for a small excess "cold" X-ray absorbing column density in an *ASCA* observation (George et al. 2000, hereafter G00). Note that this object shows large amplitude changes in $\alpha_{ox}$ (Gallagher et al. 2001, Fig. 9 there).

0923+201– *HST* did not observe C IV, and only part of the blue wing of N V was observed. However, the "valley" between N V and Ly$\alpha$ is much deeper than normally seen in AGN spectra, where the blue wing of N V generally blends into Ly$\alpha$ with only a slight drop in flux density (see all the other profiles in Figs. 1-3). The bottom of this dip at $v \sim -2500$ km s$^{-1}$ matches quite well the Ly$\alpha$ absorption system at $-2500$ km s$^{-1}$. The absorption in both Ly$\alpha$ and N V appears to include a broad, shallow component ($-4000 \lesssim v \lesssim -2000$ km s$^{-1}$) on top of a narrow unresolved core.

0947+396– BLW suggest weak C IV absorption (EW$\sim$ 0.2 Å) based on the line-peak asymmetry. Since there is no clear absorption dip in the line profile we adopt a more conservative estimate of EW=0 Å. *ROSAT* and *BeppoSAX* spectra do not find significant absorption (L97; Mineo et al. 2000, hereafter M00).

0953+414– J98 did not note intrinsic C IV absorption in this object, but Ganguly et al. (2001) did. The C IV absorption is only marginally significant, though both doublet components seem to be present. The velocity shift of $-1380$ km s$^{-1}$ found by Ganguly et al. is based on $z = 0.239$. The revised value of $z = 0.23405$ based on the peak of [O III]$\lambda$5007 (see Table 1) gives a velocity shift of only 100 km s$^{-1}$. *ROSAT* and *ASCA* spectra (L97; G00) suggest there may be a small intrinsic X-ray absorbing column density.

1011–040– BLW give EW(C IV)<1.2 Å based on the available *IUE* spectrum. However, the marginally significant absorption centered at $v = -200$ km s$^{-1}$ in C IV appears to be present in N V and Ly$\alpha$ as well. We therefore adopt EW(C IV)= 1 Å for this object, though a higher quality spectrum is obviously required to verify this result.

1049–005– The C IV absorption was noted by J98 and by Ganguly et al. (2001). The absorption is very weak, but both doublet components are clearly present.

1100+772– The C IV absorption was noted by J98 and by Ganguly et al. (2001). The absorption is rather weak but clearly present in C IV, Ly$\alpha$, and O VI. *ROSAT* and *ASCA* spectra do not reveal any intrinsic absorption (Wang, Brinkmann, & Bergeron 1996; Sambruna et al. 1999).

1115+407– The C IV absorption is weak, but both doublet components are clearly present. The N V doublet is also clearly present. *ROSAT* and *BeppoSAX* do not reveal significant intrinsic absorption (L97; M00).

1116+215– BLW suggest very weak C IV absorption (EW$\sim$ 0.1 Å) based on a feature at $v = -9500$ km s$^{-1}$. This feature is below the detection threshold of J98, and the second doublet component is not seen. If real, this system is likely to be associated with the intervening Ly$\alpha$ system at $v = -9500$ km s$^{-1}$(related to an intervening galaxy; Tripp, Lu & Savage 1998), and we therefore adopt here EW(C IV)=0 Å. A very high S/N *ROSAT* spectrum puts a strong constraint on any cold absorber (L97), and an *ASCA* spectrum suggests a weak warm absorber (G00).

1202+281– BLW give EW(C IV)=0.4 Å. This is based on the C IV line-peak asymmetry. However, inspection of the H$\beta$ profile in BG92 reveals the same asymmetry. Since H$\beta$ absorption is extremely rare, we conclude that the emission-line asymmetry is most likely not due to absorption, and adopt here EW(C IV)=0 Å. A rather high S/N *ROSAT* spectrum does not reveal any evidence for absorption (L97)

1211+143– BLW give EW(C IV)=0.5 Å. This is based on marginally significant features at $v \sim -8000$ km s$^{-1}$. The two apparent narrow C IV components are somewhat too close (400 km s$^{-1}$ apart, instead of 500 km s$^{-1}$) and are displaced by $\sim$ 200 km s$^{-1}$ from the nearest Ly$\alpha$ absorber. We conclude that the identification of this system is not secure and adopt EW(C IV)=0 Å. High S/N *ROSAT* and *ASCA* spectra do not reveal any intrinsic absorption (Fiore et al. 1994; G00).

1322+659– BLW give EW(C IV)=0.2 Å, based on a narrow absorption feature at $v = 120$ km s$^{-1}$. A similarly shaped absorption feature occurs in Ly$\alpha$, but it is centered at $v = -20$ km s$^{-1}$. The apparent C IV absorption is centered at 1808.2 Å, and it may be due to Galactic Si II $\lambda$1808.0 since the other resonance Si II lines at 1190.4 Å, 1193.3 Å, 1260.4 Å, 1304.4 Å, and 1526.7 Å are unusually strong. We therefore conservatively adopt EW(C IV)=0 Å. A *ROSAT* spectrum suggests a low-column density intrinsic neutral absorber, and an *ASCA* spectrum suggests a weak warm absorber (L97; G00).

1352+183– BLW give EW(C IV)=0.5 Å based on a narrow absorption feature at $v = -9900$ km s$^{-1}$. However, since the second C IV doublet component does not appear to be present, and the nearest possible Ly$\alpha$ absorption is at $v = -10200$ km s$^{-1}$, we conclude that this feature is most likely not due to C IV and adopt EW(C IV)=0 Å. No absorption is seen with *ROSAT* and *BeppoSAX* (L97; M00).

1402+261– Although C IV absorption is clearly seen at $v = -4600$ km s$^{-1}$, two earlier *HST* observations in 1993 (PI Tytler) and in 1994 (Turnshek et al. 1997) do not show significant absorption in C IV, providing strong evidence that the absorption is variable. No absorption is seen with *ROSAT* and *BeppoSAX* (L97; M00).

1427+480– BLW give EW(C IV)=0.03 Å based on two very weak features at $v = -100$ km s$^{-1}$ and $v = 400$ km s$^{-1}$, and a weak Ly$\alpha$ absorption feature at $v = 0$ km s$^{-1}$. Since the amplitudes of these features are comparable to the noise we adopt here EW(C IV)=0 Å. No absorption is seen with *ROSAT* (L97).

1512+370– BLW give EW(C IV)=0.2 Å based on two apparently significant features at $v = 250$ km s$^{-1}$ and $v = 800$ km s$^{-1}$. However, since there is no clear corresponding Ly$\alpha$ feature we adopt EW(C IV)=0 Å here. J98 and Ganguly et al. (2001) also do not identify these features as C IV absorption. No absorption is seen with *ROSAT* and *BeppoSAX* (L97; M00).

1543+489– BLW give EW(C IV)=0.4 Å based on an apparently very broad and very shallow absorption dip at the C IV line peak ($v = -1000$ km s$^{-1}$ to $-3000$ km s$^{-1}$). However, since we cannot rule out a peculiar line profile in this rather extreme EV1 object (BG92), we adopt EW(C IV)=0 Å here.

2214+139– BLW give EW(C IV)< 1.2 Å based on the available *IUE* spectrum. However, the peak of N V appears to be red-shifted by $\sim$ 1000 km s$^{-1}$, which is highly unusual and may imply absorption of the blue wing of N V. Some absorption may be present in C IV at $v = -1000$ km s$^{-1}$, though Ly$\alpha$ shows no evidence for absorption. We tentatively estimate a marginally significant EW(C IV)=1.1 Å and use a different symbol for this object throughout the paper.

2251+113– BLW give EW(C IV)=0.8 Å based on a very deep resolved C IV doublet at $v = 0$ km s$^{-1}$. Here we identify additional absorption extending up to $v = -5000$ km s$^{-1}$, which increases EW(C IV) to 3.5 Å (see also the comment in §6.4 of Ganguly et al. 2001). The velocity shift of 610 km s$^{-1}$ found by Ganguly et al. is based on $z = 0.323$. The revised value of $z = 0.32553$ (see Table 1) gives a velocity shift of 0 km s$^{-1}$.

## APPENDIX

### B. OBJECTS WITH EW(C IV)< 0.1 Å

For the sake of completeness we list the 28 objects where we find intrinsic EW(C IV)< 0.1 Å. This limit is based on C IV, Ly$\alpha$, and N V. In objects where these three lines are not all available we list in parentheses the line which was available and used to constrain the UV absorption. The "no UV absorption" sample includes the following objects: PG 0003+158, PG 0003+199, PG 0026+129,

PG 0052+251 (C IV), PG 0947+396, PG 1103−006, PG 1116+214, PG 1121+422 (C IV), PG 1202+281, PG 1211+143, PG 1216+069, PG 1226+023, PG 1259+593, PG 1302−102, PG 1307+085 (C IV), PG 1322+659, PG 1352+183, PG 1415+451, PG 1416−129, PG 1427+480, PG 1440+356, PG 1444+407, PG 1512+370, PG 1534+580 (Ly$\alpha$), PG 1543+489, PG 1545+210, PG 1612+261 (C IV), PG 1626+554.

## REFERENCES


Arav, N. 1997, in ASP Conf. Ser. 128: Mass Ejection from Active Galactic Nuclei, eds. N. Arav, I. Shlosman, and R. J. Weymann, (ASP Press: San Francisco), 208

Arav, N., Li, Z., & Begelman, M. C. 1994, ApJ, 432, 62

Arav, N. et al. 2001, ApJ, 561, 118

Becker, R. H., White, R. L., Gregg, M. D., Brotherton, M. S., Laurent-Muehleisen, S. A., & Arav, N. 2000, ApJ, 538, 72

Becker, R. H. et al. 2001, ApJS, 135, 227

Begelman, M., de Kool, M., & Sikora, M. 1991, ApJ, 382, 416

Boller, T., Brandt, W. N., & Fink, H. 1996, A&A, 305, 53

Boroson, T. A. 2002, ApJ, in press (astro-ph/0109317)

Boroson, T. A., & Green, R. F. 1992, ApJS, 80, 109 (BG92)

Boroson, T. A., & Meyers, K. A. 1992, ApJ, 397, 442

Brandt, W. N., & Boller, Th. 1999, in Structure and Kinematics of Quasar Broad Line Regions, eds. Gaskell, C. M. Brandt, W. N., Dietrich, M., Dultzin-Hacyan, D., Eracleous, M. (ASP Press: San Francisco), 265

Brandt, W. N., Laor, A., & Wills, B. J. 2000, ApJ, 528, 637 (BLW)

Brotherton, M. S., Tran, H. D., Becker, R. H., Gregg, M. D., Laurent-Muehleisen, S. A., & White, R. L. 2001, ApJ, 546, 775

Crenshaw, D. M., Kraemer, S. B., Boggess, A., Maran, S. P., Mushotzky, R. F., & Wu, C. 1999, ApJ, 516, 750

Ferrarese, L., Pogge, R. W., Peterson, B. M., Merritt, D., Wandel, A., & Joseph, C. L. 2001, ApJ, 555, L79

Gallagher, S. C., Brandt, W. N., Sambruna, R. M., Mathur, S., & Yamasaki, N. 1999, ApJ, 519, 549

Gallagher, S. C., Brandt, W. N., Laor, A., Elvis, M., Mathur, S., Wills, B. J., & Iyomoto, N. 2001, ApJ 546, 795

Ganguly, R., Bond, N. A., Charlton, J. C., Eracleous, M., Brandt, W. N., & Churchill, C. W. 2001, ApJ, 549, 133

Gebhardt, K. et al. 2000, ApJ, 543, L5

George, I. M., Nandra, K., Laor, A., Turner, T. J., Fiore, F., Netzer, H., & Mushotzky, R. F. 1997, ApJ, 491, 508

George, I. M., Turner, T. J., Yaqoob, T., Netzer, H., Laor, A., Mushotzky, R. F., Nandra, K., & Takahashi, T. 2000, ApJ, 531, 52 (G00)

Goodrich, R. W. 1997, ApJ, 474, 606

Green, P. J. et al. 1995, ApJ, 450, 51

Green, P. J. & Mathur, S. 1996, ApJ, 462, 637

Green, P. J., Aldcroft, T. L., Mathur S., Wilkes, B. J., Elvis, M. 2001, ApJ, in press

Hall, P., 2001, in Mass Outflow in Active Galactic Nuclei: New Perspectives, eds. D. M. Crenshaw, S. B. Kraemer, & I. M. George, in press (astro-ph/0107182)

Hamann, F. 1998, ApJ, 500, 798

Hamann, F., Barlow, T. A., & Junkkarinen, V. 1997, ApJ, 478, 87

Jannuzi, B. T. et al. 1996, ApJ, 470, L11

Jannuzi, B. T. et al. 1998, ApJS, 118, 1 (J98)

Kaspi, S., Smith, P. S., Netzer, H., Maoz, D., Jannuzi, B. T., & Giveon, U. 2000, ApJ, 533, 631

Kaspi, S., Brandt, W. N., Netzer, H., George, I. M., Chartas, G., Behar, E., Sambruna, R. M., Garmire, G. P., & Nousek, J. A. 2001, ApJ, 554, 216

Kendall, M., & Stuart, A. 1977, The Advanced Theory of Statistics, Vol. 2 (4th ed.; New York: Macmillian)

Kopko, M., Turnshek, D. A., & Espey, B. R. 1994, IAU Symp. 159: Multi-Wavelength Continuum Emission of AGN, 159, 450

Korista, K. T. et al. 1992, ApJ, 401, 529

Kraemer, S. B., et al. 2001, ApJ, 551, 671

Krolik, J. H. 2001, ApJ, 551, 72

Krolik, J. H. & Voit, G. M. 1998, ApJ, 497, L5

Kuraszkiewicz, J., Wilkes, B. J., Brandt, W. N., & Vestergaard, M. 2000, ApJ, 542, 631

Kwan, J. 1990, ApJ, 353, 123

Laor, A. 1998, ApJ, 505, L83

Laor, A. 2000, NewA Rev, 44, 503

Laor, A. & Draine, B. T. 1993, ApJ, 402, 441

Laor, A., Fiore, F., Elvis, M., Wilkes, B. J., & McDowell, J. C. 1997, ApJ, 477, 93 (L97)

Mathur, S. et al. 2000, ApJ, 533, L79

Menou, K., et al. 2001, ApJ, 561, 645

Mineo, T. et al. 2000, A&A, 359, 471 (M00)

Murray, N. & Chiang, J. 1995, ApJ, 454, L105

Murray, N., Chiang, J., Grossman, S. A., & Voit, G. M. 1995, ApJ, 451, 498

Netzer, H., & Laor, A. 1993, ApJ, 404, L51

Netzer, H. 1990 in Active Galactic Nuclei, ed. T. J.L. Courvoisier & M. Mayor (Berlin: Springer), 57

Neugebauer, G., et al. 1987, ApJS, 63, 615

Peterson, B. M. & Wandel, A. 2000, ApJ, 540, L13

Richards, G. T., York, D. G., Yanny, B., Kollgaard, R. I., Laurent-Muehleisen, S. A., & vanden Berk, D. E. 1999, ApJ, 513, 576

Risaliti, G., Marconi, A., Maiolino, R., Salvati, M., & Severgnini, P. 2001, A&A, 371, 37

Sambruna, R. M., Eracleous, M., & Mushotzky, R. F. 1999, ApJ, 526, 60

Savage, B. D. et al. 2000, ApJS, 129, 563

Schmidt, M., & Green, F. G. 1983, ApJ, 269, 352

Scoville, N., & Norman, C. 1995, ApJ, 451, 510

Turnshek, D. A., Monier, E., Sirola, C. J., & Espey, B. R. 1997, ApJ, 476, 40

Tripp, T. M., Lu, L., & Savage, B. D. 1998, ApJ, 508, 200

Wang, T., Brinkmann, W., & Bergeron, J. 1996, A&A, 309, 81

Wang, T. G., Brinkmann, W., Matsuoka, M., Wang, J. X., & Yuan, W. 2000, ApJ, 533, 113

Wills, B. J., Laor, A., Brotherton, M. S., Wills, D., Wilkes, B. J., Ferland, G. J., & Shang, Z. 1999, ApJ, 515, L53

Weymann, R. J., Turnshek, D. A., & Christiansen, W. A. 1985, in Astrophysics of Active Galaxies and Quasi-Stellar Objects, ed. J. S. Miller (Mill Valley, CA: University Science Books), 333

Weymann, R. J., Morris, S. L., Foltz, C. B., & Hewett, P. C. 1991, ApJ, 373, 23

Zheng, W., et al. 2001, ApJ, 562, 152

TABLE 1

C IV Absorption Parameters for BG92 Quasar Sample

| Object name | $z^a$ | $M_V^b$ | $\nu L_\nu^c$ | $\alpha_{ox}$ | EW([O III]) (Å) | EW(C IV) (Å) | $v_{\rm max}$ (km s$^{-1}$) | $v_{\tau,\rm max}$ (km s$^{-1}$) |
|---|---|---|---|---|---|---|---|---|
| 0007+106[d] | 0.0894 | −23.85 | 44.77 | −1.43 | 42 | 0.8 | 360 | 360 |
| 0043+039[e] | 0.3859 | −26.16 | 45.49 | < −2.00 | 1 | 22.3 | 19000 | 11000 |
| 0050+124 | 0.0609 | −23.77 | 44.58 | −1.56 | 22 | 0.4 | 1850 | 1850 |
| 0844+349[d] | 0.0644 | −23.31 | 44.46 | −1.54 | 8 | 0.6 | −100 | −100 |
| 0923+201[d] | 0.1929 | −24.56 | 45.14 | −1.57 | 7 | 0.8 | 2700 | 2700 |
| 0953+414 | 0.2340 | −25.65 | 45.47 | −1.50 | 18 | 0.1 | 100 | 100 |
| 1001+054 | 0.1610 | −24.07 | 44.81 | −2.13 | 7 | 11.8 | 10000 | 6150 |
| 1004+130[f] | 0.2404 | −25.97 | 45.47 | < −2.01 | 6 | 16.6 | 12000 | 6800 |
| 1011−040[f] | 0.0584 | −22.70 | 44.22 | −2.01 | 15 | 1.0: | 3000: | 2000: |
| 1049−005 | 0.3596 | −25.93 | 45.54 | −1.56 | 55 | 0.3 | 4050 | 4050 |
| 1100+772 | 0.3115 | −25.86 | 45.54 | −1.39 | 41 | 0.4 | 750 | 750 |
| 1114+445 | 0.1438 | −24.01 | 44.67 | −1.62 | 17 | 4.0 | 800 | 250 |
| 1115+407 | 0.1542 | −23.74 | 44.55 | −1.45 | 6 | 0.3 | −200 | −200 |
| 1126−041[f] | 0.0601 | −23.00 | 44.34 | −2.13 | 19 | 5.8 | 3300 | 2000 |
| 1309+355 | 0.1825 | −24.76 | 44.92 | −1.71 | 19 | 2.2 | 1450 | 900 |
| 1351+640 | 0.0880 | −24.08 | 44.78 | −1.78 | 31 | 5.3 | 2300 | 900 |
| 1402+261[e] | 0.1643 | −24.48 | 45.04 | −1.58 | 1 | 0.7 | 4600 | 4600 |
| 1404+226[e] | 0.0978 | −22.93 | 44.13 | −1.55 | 7 | 1.5 | 2400 | 1800 |
| 1411+442 | 0.0898 | −23.54 | 44.52 | −2.03 | 15 | 10.3 | 4100 | 2000 |
| 1425+267 | 0.3635 | −26.18 | 45.22 | −1.63 | 36 | 2.1 | 1600 | 800 |
| 1535+547[d,g] | 0.0388 | −22.15 | 43.82 | < −2.17 | 16 | 3.9 | 1400 | 400 |
| 1700+518 | 0.2892 | −26.44 | 45.51 | < −2.29 | 0 | 94 | 31000 | 12000 |
| 1704+608 | 0.3721 | −26.38 | 45.61 | −1.62 | 27 | 2.4 | 2500 | 1750 |
| 2112+059 | 0.4597 | −27.26 | 46.13 | −2.11 | 0 | 26.7 | 24000 | 18400 |
| 2130+099 | 0.0631 | −23.23 | 44.62 | −1.47 | 20 | 0.6 | 1550 | 1550 |
| 2214+139[f] | 0.0657 | −23.39 | 44.46 | −2.02 | 9 | 1.1: | 2000: | 1000: |
| 2251+113 | 0.3255 | −26.24 | 45.63 | −1.86 | 19 | 3.5 | 5000 | 2950 |
| 2308+098 | 0.4336 | −26.24 | 45.62 | −1.35 | 17 | 0.2 | 0 | 0 |

[a] Kindly provided by T. A. Boroson.
[b] Taken from BG92.
[c] In units of log ergs s$^{-1}$, based on $f_\nu$ at rest frame 3000 Å from Neugebauer et al. (1987), calculated for $H_0$ = 80 km s$^{-1}$ Mpc$^{-1}$, $\Omega_0$ = 1.0.
[d] Based on Ly$\alpha$.
[e] No Galactic absorption lines were available for calibration. The velocity scale may be off by $\sim$ 300 km s$^{-1}$.
[f] Based on a low spectral resolution ($\sim$ 1000 km s$^{-1}$) *IUE* spectrum.
[g] The upper limit on $\alpha_{ox}$ is from Gallagher et al. (2001).
: Marginally significant results.
Note: the following five objects have a non zero balnicity index (Weymann et al. 1991): PG 0043+039, 1210 km s$^{-1}$; PG 1001+054, 684 km s$^{-1}$; PG 1004+130, 417 km s$^{-1}$; PG 1700+518, 13140 km s$^{-1}$; PG 2112+059, 1520 km s$^{-1}$.

TABLE 2

Estimated Statistics of Obscuring Material Covering Factors

<table>
<tr><th></th><th>EW(C IV)</th><th>$M_{\rm [O\ III]} < -27$</th><th>$M_{\rm [O\ III]} > -27$</th></tr>
<tr><td>Clear</td><td>< 0.1 Å</td><td>$\sim$ 57% (17/30)</td><td>$\sim$ 40% (11/26)</td></tr>
<tr><td>Weak absorption</td><td>0.1–1 Å</td><td>$\sim$ 20% (6/30)</td><td rowspan="2">$\sim$ 25% (6/26)</td></tr>
<tr><td>Intermediate absorption</td><td>1–10 Å</td><td>$\sim$ 20% (6/30)</td></tr>
<tr><td>Strong absorption</td><td>> 10 Å</td><td>$\sim$ 3% (1/30)</td><td>$\sim$ 35% (9/26)</td></tr>
</table>

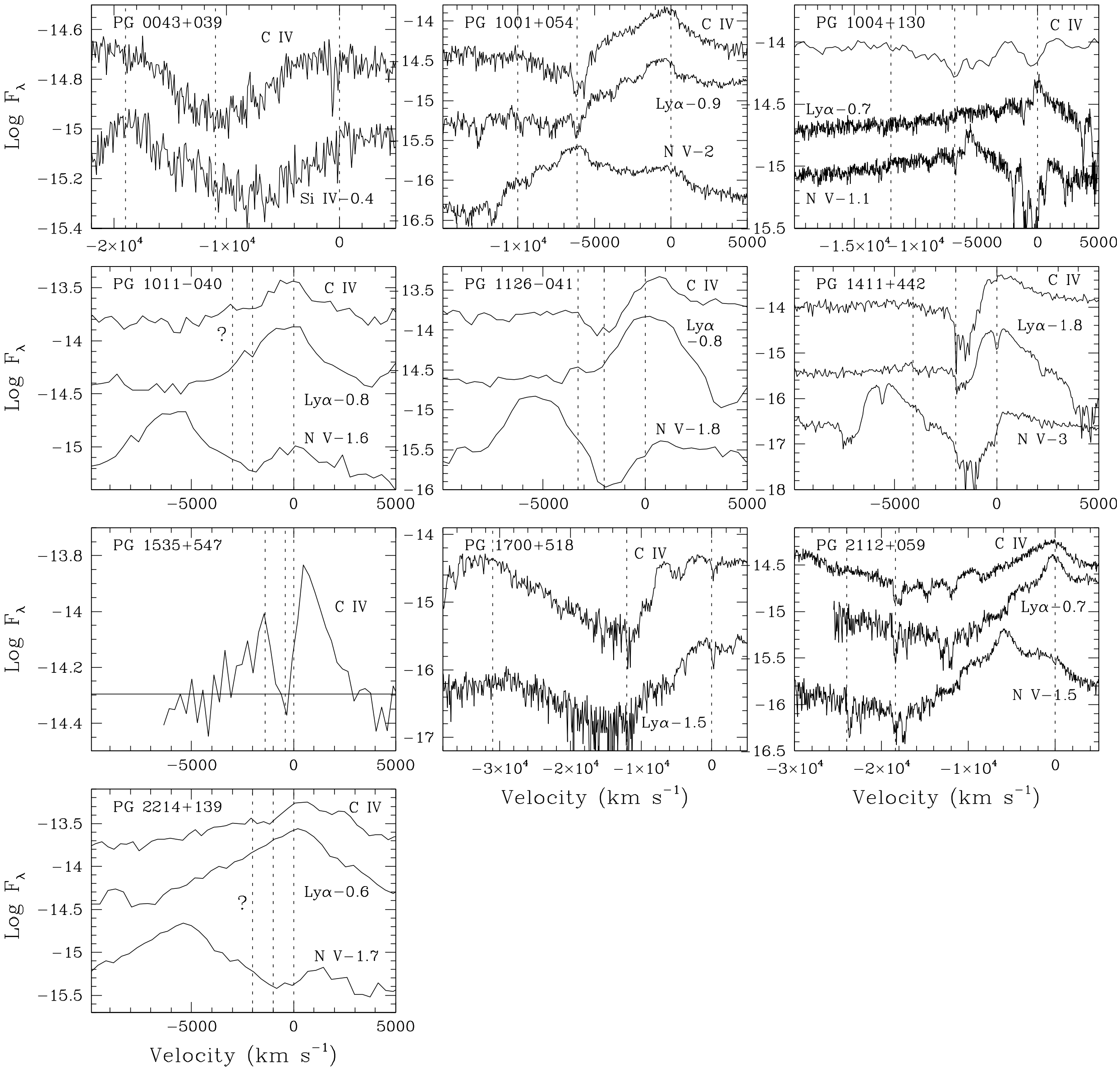


FIG. 1.— The C IV, Ly$\alpha$, and N V absorption-line profiles for the SXWQs (not all lines are available for all objects). The flux density is in units of observed ergs s$^{-1}$ Å$^{-1}$ cm$^{-2}$. The three vertical dashed lines in each panel indicate $v = 0$ km s$^{-1}$, defined with respect to the shorter wavelength doublet component, the velocity of maximum absorption, $v_{\tau,\max}$ and the maximum velocity of absorption, $v_{\max}$. The Ly$\alpha$ and N V profiles are shifted downward for clarity by the amount indicated next to the line label. Note that the significance of the absorption in PG 1011−040 and PG 2214+139 is only marginal.

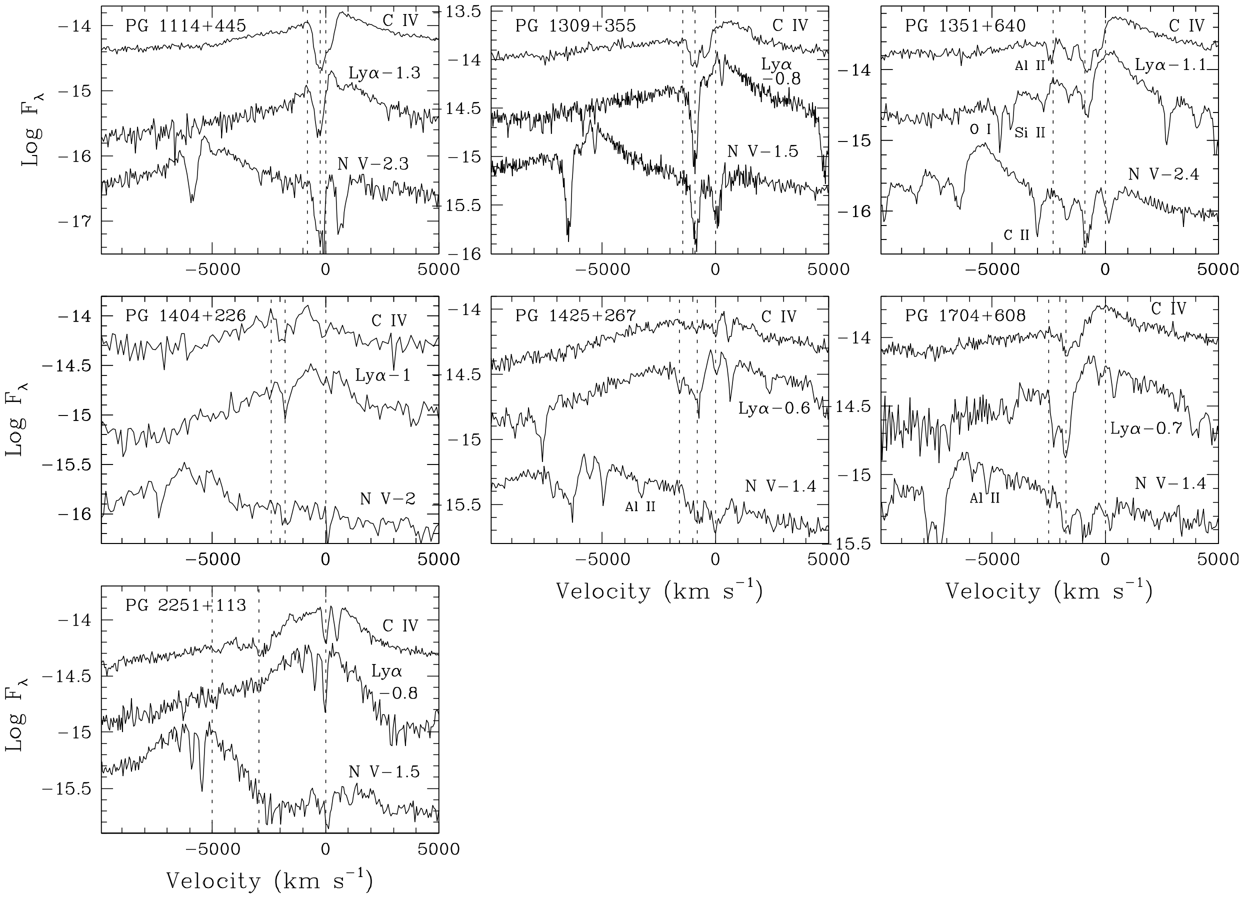


FIG. 2.— As in Figure 1 for the objects with intermediate-strength C IV absorption (1 Å<EW<10 Å) that are not SXWQs. Note that since the absorption lines are generally narrow, it is possible to resolve the longer wavelength doublet component of C IV at 500 km s$^{-1}$, and that of N V at 960 km s$^{-1}$. Narrow absorption features due to Galactic absorption are designated.

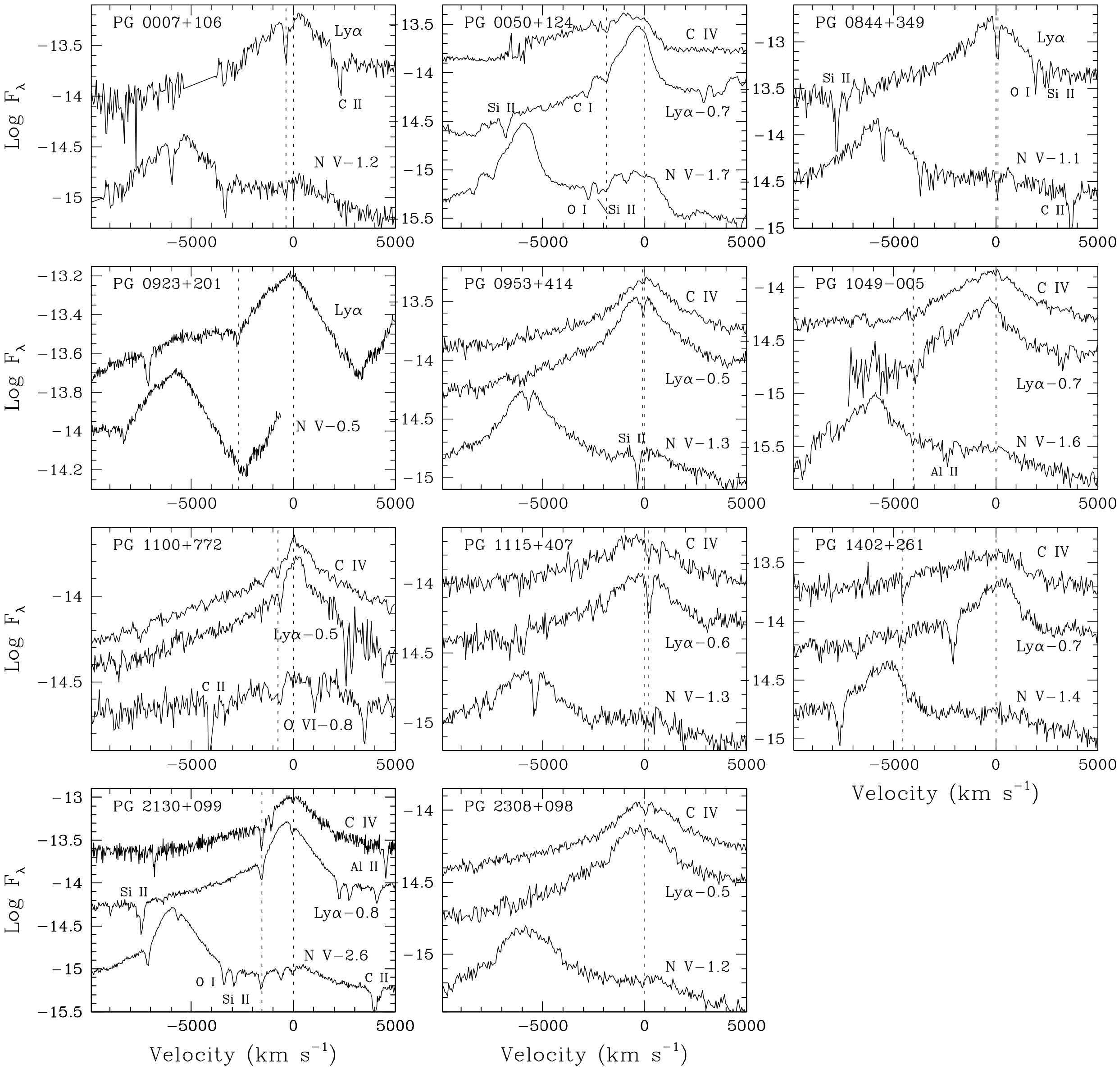


FIG. 3.— As in Figures 1 and 2 for the objects with weak C IV absorption (EW<1 Å). Since the absorption features are not resolved, only $v_{\tau,\max}$ is indicated.

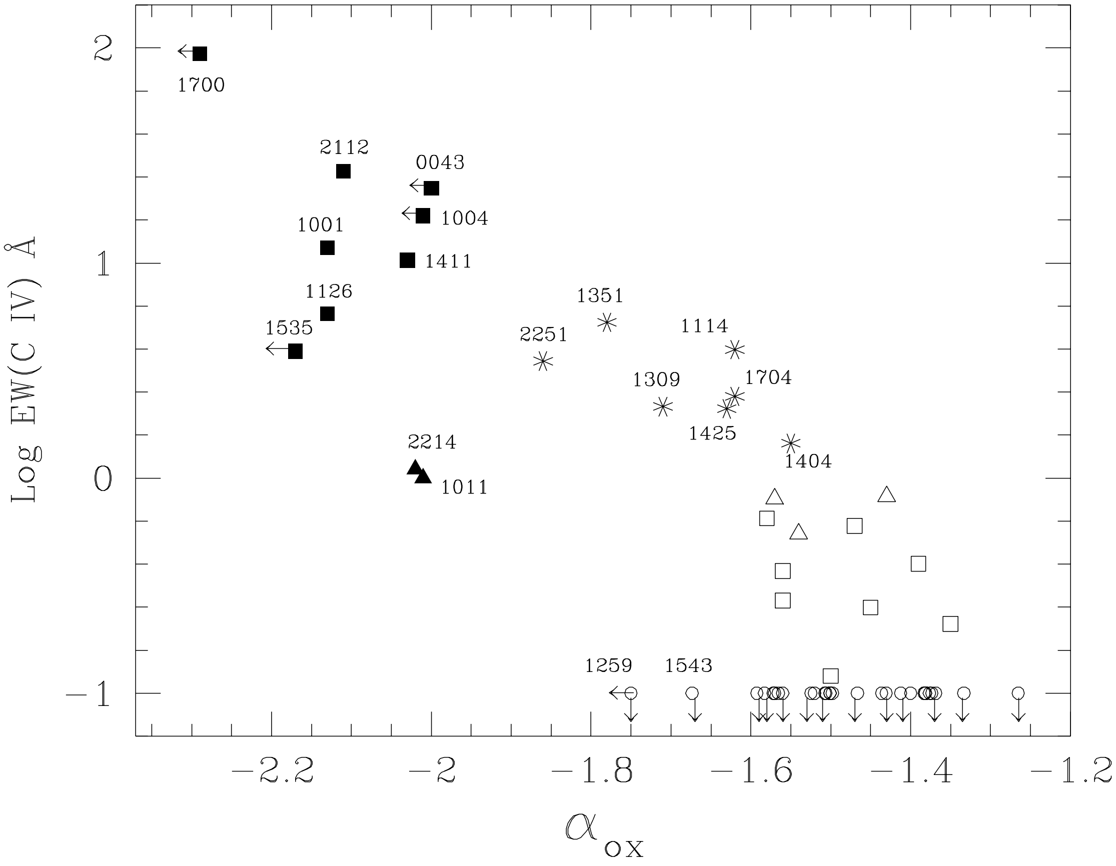


FIG. 4.— The absorption EW(C IV) vs. $\alpha_{ox}$ relation for the BG92 AGN. Filled squares are SXWQs, stars are non-SXWQs with intermediate C IV absorption (1 Å<EW<10 Å), open squares are AGN with weak C IV absorption (EW<1 Å), and open triangles have weak Ly$\alpha$ absorption. Open circles at log EW(C IV)=−1 indicate objects with no detectable absorption. Filled triangles mark the two SXWQs where the absorption is only marginally significant. Some objects are designated by the right ascension part of their name. Note that AGN with intermediate absorption have a steeper $\alpha_{ox}$ than AGN with weak absorption, and all AGN with strong absorption (EW>10 Å) are SXW.

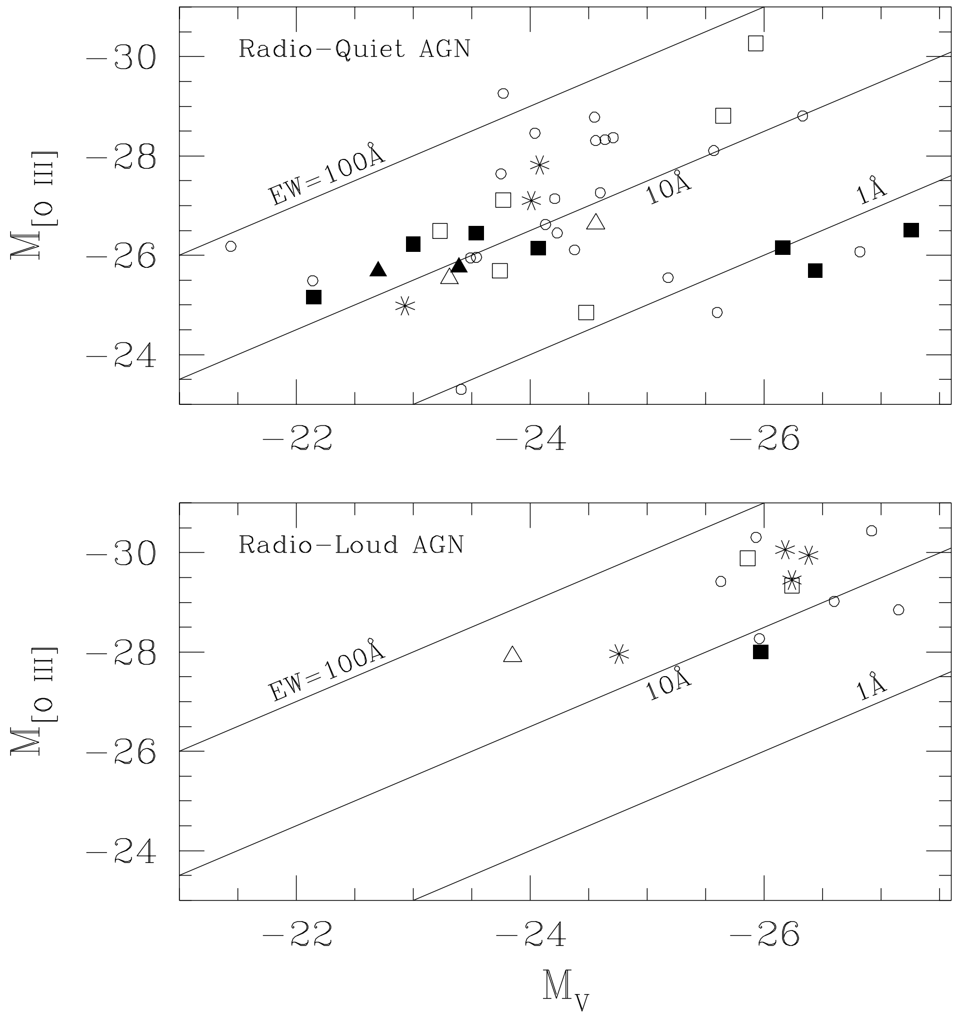


FIG. 5.— The $M_{[\rm O\ III]}$ vs. $M_V$ relation for the radio-quiet and radio-loud BG92 AGN. Symbols are as in Fig. 4, and open circles mark the 28 objects with no C IV absorption. The diagonal solid lines indicate constant [O III] EW. The distribution of AGN with intermediate/weak UV absorption is similar to AGN with no absorption, but SXWQs have preferentially low [O III] luminosity.

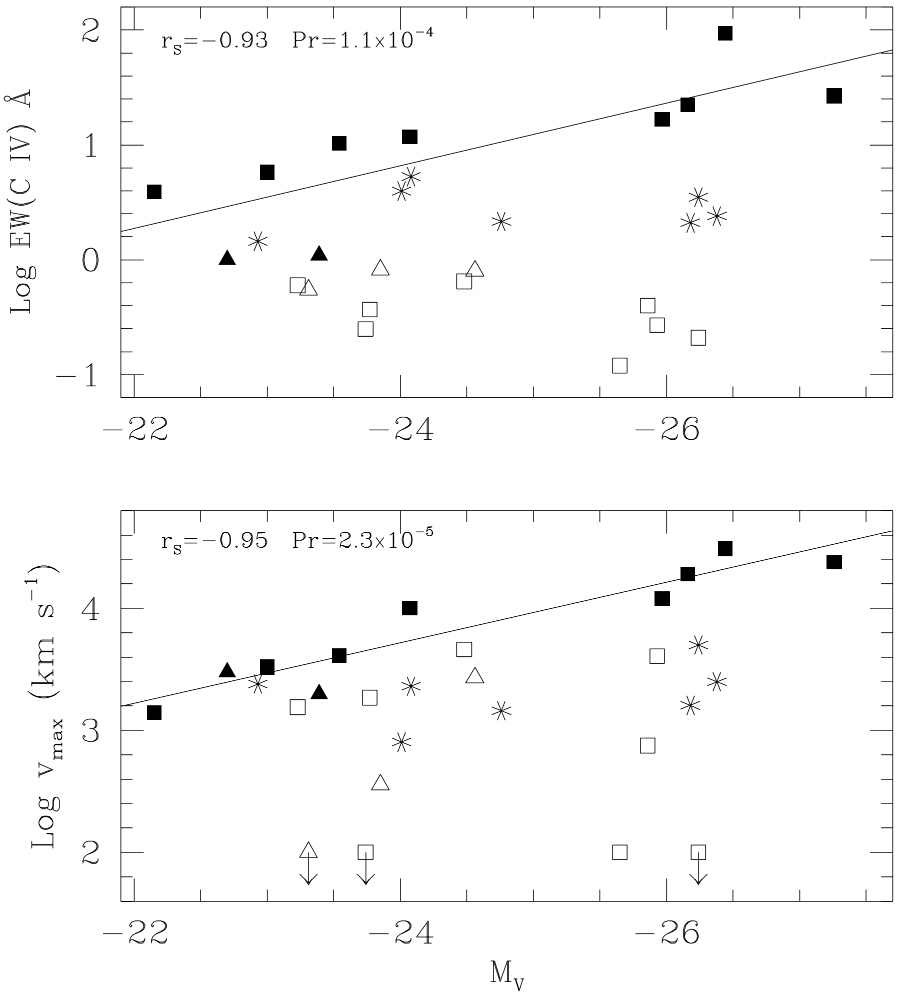


FIG. 6.— The luminosity dependence of EW(C IV) and of $v_{max}$. SXWQs have higher EW(C IV) and $v_{max}$ than other absorbed quasars at any given luminosity, and both parameters of the SXWQs are significantly correlated with luminosity. The Spearman correlation coefficient for the SXWQs ($r_S$) and its significance level (Pr) are indicated in each panel. The solid line in each panel is a least-squares fit to the SXWQs. Note the very tight relation between $v_{max}$ and $M_V$ for the SXWQs ($v_{max} \propto L^{0.62\pm0.08}$), as qualitatively expected for some radiation-pressure driven outflow scenarios.

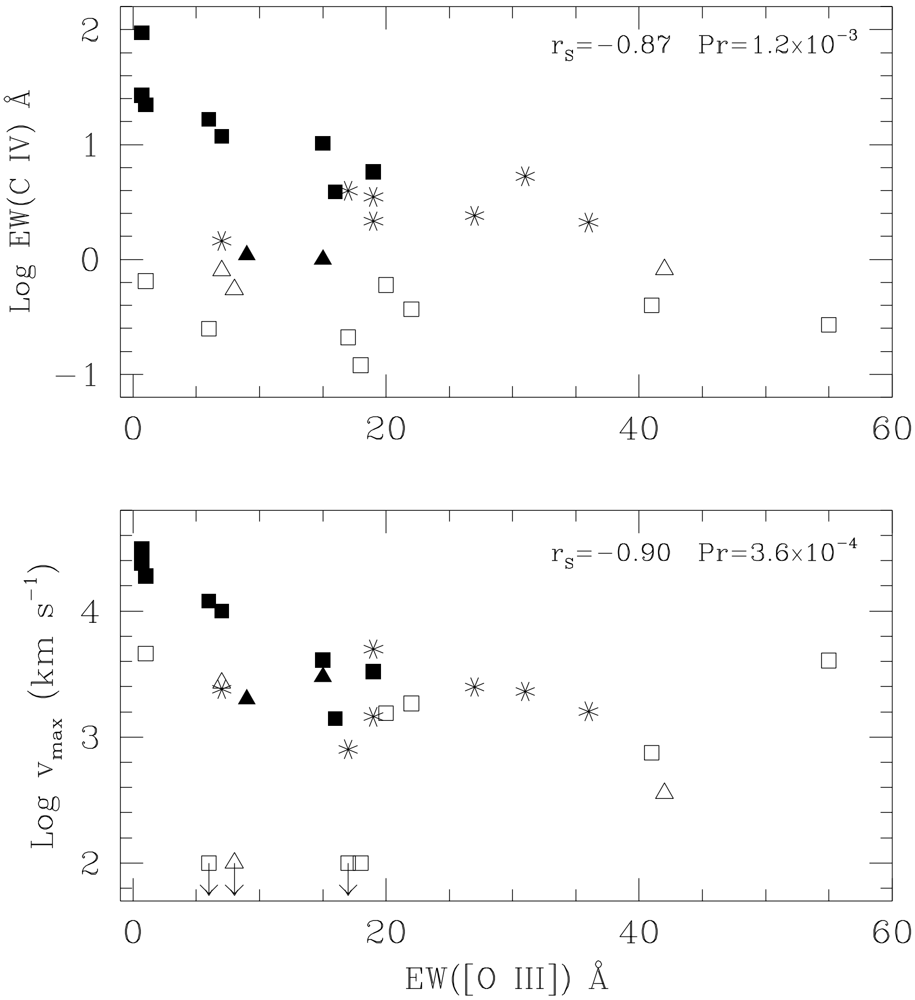


FIG. 7.— The dependence of absorption EW(C IV) and $v_{\rm max}$ on EW([O III]). Both parameters for the SXWQs are significantly correlated with EW([O III]). The values of $r_S$ and Pr for the SXWQs are indicated in each panel.

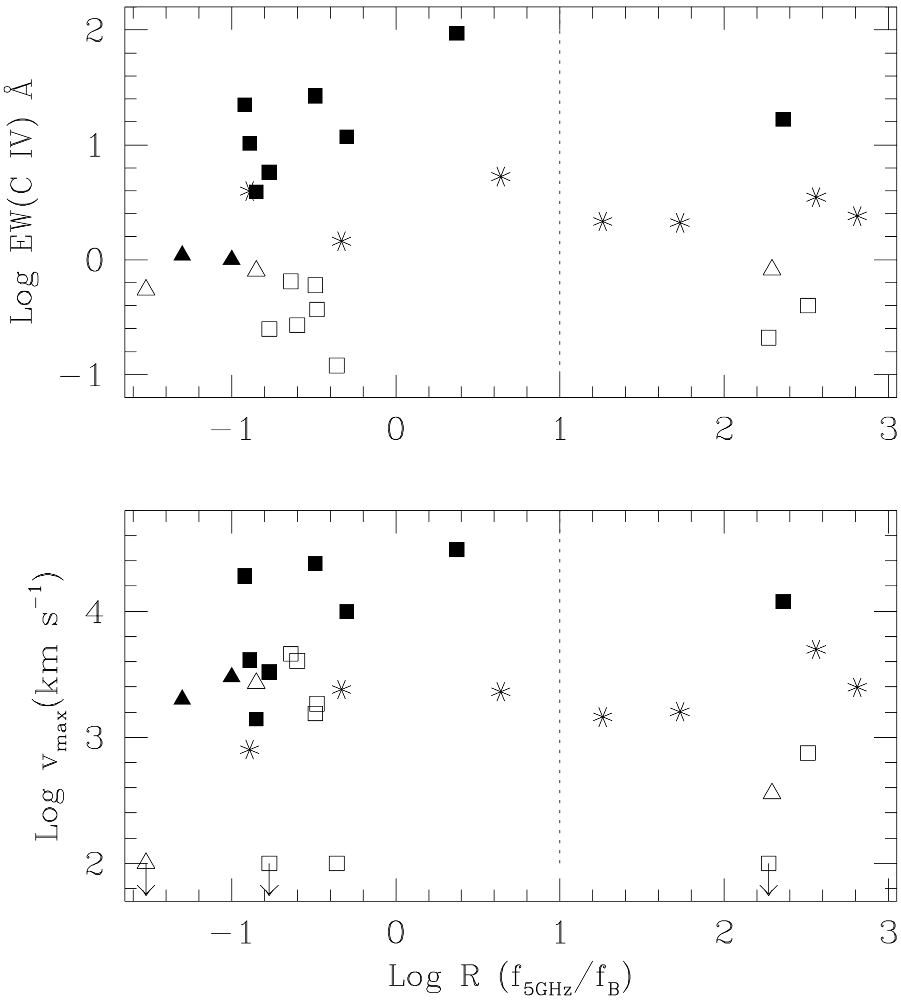


FIG. 8.— The radio-loudness dependence of EW(C IV) and of $v_{max}$. The vertical dashed line separates radio-quiet and radio-loud AGN. There may be a hint for somewhat lower EW(C IV) and $v_{max}$ in radio-loud AGN, but the observed differences are not formally significant (see text).

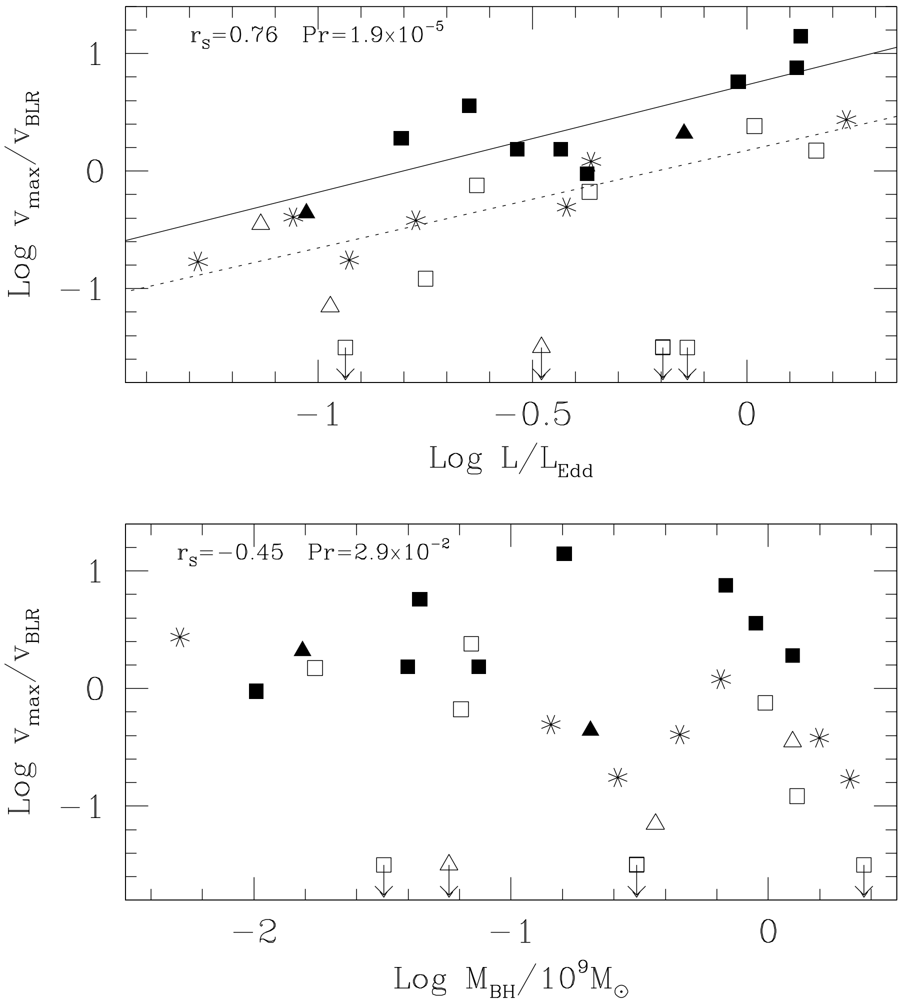


FIG. 9.— The dependence of $v_{\rm max}/v_{\rm BLR}$ on the estimated $L/L_{\rm Edd}$ and $M_{\rm BH}$. Note the rather strong correlation between $v_{\rm max}/v_{\rm BLR}$ and $L/L_{\rm Edd}$ for all absorbed objects, but the only marginal correlation with $M_{\rm BH}$. Upper limits represent objects with no significant outflows ($v_{\rm max} \leq 100$ km s$^{-1}$), which are excluded from the analysis. The values of $r_{\rm S}$ and Pr for the 24 AGN with significant outflows are indicated in each panel. The solid line is a least-squares fit for the 10 SXWQs, which gives $v_{\rm max}/v_{\rm BLR} \propto (L/L_{\rm Edd})^{0.91\pm0.24}$, and the dotted line is a fit for the 14 non-SXWQs, which gives $v_{\rm max}/v_{\rm BLR} \propto (L/L_{\rm Edd})^{0.83\pm0.16}$.